Semirelativistic study of the semileptonic decays of B_q mesons to orbital excited heavy tensors

Wen-Yuan Ke,[1,2,3,†] Su-Yan Pei,[1,2,3] Tianhong Wang,[4] and Guo-Li Wang[1,2,3,*]

[1]*Department of Physics, Hebei University, Baoding 071002, China*
[2]*Hebei Key Laboratory of High-Precision Computation and Application of Quantum Field Theory, Baoding 071002, China*
[3]*Hebei Research Center of the Basic Discipline for Computational Physics, Baoding 071002, China*
[4]*School of Physics, Harbin Institute of Technology, Harbin 150001, China*

(Received 4 December 2023; accepted 27 February 2024; published 26 March 2024)

Based on the method of solving the complete Salpeter equation, we study the semileptonic decays of a 0^- heavy meson to $1P$, $2P$, or $3P$ heavy-tensor mesons, $B_q \to (\bar{c}q)(nP)\ell^+\nu_\ell$ ($q = u, d, s, c; n = 1, 2, 3$). The obtained branching ratio of $\mathcal{B}(B \to D_2^\star(2460)\ell^+\nu_\ell)$ agrees with the experimental data. We predict $\mathcal{B}(B_s^0 \to D_{s2}^{\star -}(1P)\ell^+\nu_\ell) = 3.76 \times 10^{-3}$ and $\mathcal{B}(B_c^+ \to \chi_{c2}(1P)\ell^+\nu_\ell) = 1.82 \times 10^{-3}$. The branching ratios of decays to $2P$ and $3P$ final states are found to be very small. The ratios $\mathcal{R}(\bar{D}_2^{\star 0}) = 0.045$, $\mathcal{R}(D_{s2}^\star) = 0.048$ and $\mathcal{R}(\chi_{c2}) = 0.059$ are also obtained. This study focuses on the contribution of relativistic corrections. The wave function of the pseudoscalar includes nonrelativistic S-wave and relativistic P-wave. While for a tensor, it contains nonrelativistic P-wave and relativistic P-, D-, and F-waves in its wave function. We find the individual contributions of relativistic partial waves are significant in the decay $B \to D_2^\star(2460)\ell^+\nu_\ell$, but the overall contribution of the relativistic effect is 24.4%, which is small due to cancellation. Similarly, for the decay $B_s^0 \to D_{s2}^{\star -}(1P)\ell^+\nu_\ell$, the contribution of the relativistic effect is 28.8%. While for $B_c^+ \to \chi_{c2}(1P)\ell^+\nu_\ell$, the individual contributions of relativistic partial waves and the overall relativistic correction are both small, the later of which is 22.1%.

DOI: 10.1103/PhysRevD.109.053004

I. INTRODUCTION

In the past few years, the semileptonic decays of bottom mesons induced by $b \to c$ have attracted a lot of research interest both in theory [1–5] and in experiment [6–11], since such decays are important for the studies of the Cabibbo-Kobayashi-Maskawa (CKM) matrix element V_{cb} [12,13], CP violation [14,15], probing new physics [16,17], etc. So far, many processes have been extensively studied, such as the semileptonic decays of B to D or $D^\star$. However our knowledge on the final state being an orbitally excited state is still insufficient. For example, there is the long-lived "1/2 vs 3/2" puzzle [18–22] in B semileptonic decays to orbitally excited states.

Among the orbitally excited states, the 2^+ tensor meson is a very complex one. There are significant differences between theoretical results on $B \to D_2^\star(2460)\ell^+\nu_\ell$, a few results are in good agreement with experimental data, see Table IV in this article for details. The relativistic correction of an excited state is greater than that of the ground state [23], so one possible reason for the inconsistency between theory and experiment is that the relativistic correction was not well-considered. Therefore, in this article, we will give a semirelativistic study of the semileptonic decays, $B_q \to (\bar{c}q)(nP)\ell^+\nu_\ell$ $(q = u, d, s, c; n = 1, 2, 3)$, where B_q is a pseudoscalar meson, and the final meson $(\bar{c}q)$ is a tensor meson. The processes with highly excited $2P$ and $3P$ final states are also included, as we know almost nothing about them.

In this paper, we will solve the instantaneous Bethe-Salpeter (BS) equation [24], which is also called Salpeter equation [25], to obtain the Salpeter wave functions for pseudoscalar and tensor mesons. Compared with the nonrelativistic Schrödinger equation, the BS equation is a relativistic dynamic equation for bound states. As it is very complicated, we have to make approximation before solving it. The Salpeter equation is its instantaneous version, and the instantaneous approximation is suitable for heavy mesons. Due to instantaneous approximation, this method is no longer strictly relativistic, but a semirelativistic approach. We have solved the complete Salpeter equation without further approximations [26,27]. Since the

*Corresponding author: wgl@hbu.edu.cn
†20218015001@stumail.hbu.edu.cn

Salpeter equation itself does not provide the form of wave functions, we give the general expression of the Salpeter wave function for a meson according to its J^P quantum number, where the unknown radial wave functions are the solution of Salpeter equation. The Salpeter equations satisfied by mesons with different J^P need to be solved separately, see Ref. [28] for example.

It is known that some particles are not pure wave states, such as $\psi(3770)$ which is the $S-D$ mixing state [29]. In our method, a meson wave function contains different partial waves, each of which has the same J^P. It is found that [30], in our semirelativistic method, or any complete-relativistic method, similar conclusions applies to all particles, that is, all particles are not composed of pure waves, but contain other partial waves in addition to the main one. The main wave provides the nonrelativistic contribution, while others give relativistic corrections. Taking B_c meson as an example, the S-wave is its main wave which is nonrelativistic, while P-wave is the relativistic correction term [30].

Although we can calculate the ratios of different partial waves, which reflect the relativistic effect [30], they do not represent the size of the relativistic effect in the transition it participates in. In a transition process, it is necessary to calculate the overlapping integral of the initial and final-state wave functions. In this case, the relativistic correction becomes complex and requires careful study. The main contribution may not necessarily come from the nonrelativistic partial wave, but may come from the relativistic ones. This phenomenon motivates us to study the role of various partial waves in different decays. Previously, we have studied the contribution of various partial waves in strong [31] and electromagnetic transitions [32,33]. In this article, we will study their performance in the weak transition.

In Sec. II, we introduce the Bethe-Salpeter equation and its instantaneous version, that is, the Salpeter equation. In Sec. III, the wave functions including different partial waves of initial 0^- and final 2^+ mesons are given. We also show the details to solve the Salpeter equation of 2^+ state. In Sec. IV, taking the semileptonic decay $B^+ \to \bar{D}_2^\star(2460)^0\ell^+\nu_\ell$ as an example, we show with our method how to calculate the transition matrix element. In Sec. V, we present the ratios of different partial waves in the wave functions of 0^- and 2^+ mesons, and the results of semileptonic bottom meson decays. The contributions of different partial wave and discussions are also given.

II. INTRODUCTION OF BETHE-SALPETER EQUATION AND SALPETER EQUATION

The BS equation is Lorentz covariant within the framework of quantum field theory, which describes the relativistic two-body bound state. The BS equation for a bound state composed of quark 1 and antiquark 2 is generally expressed as

$$(\not{p}_1 - m_1)\chi_P(q)(\not{p}_2 + m_2) = i\int \frac{d^4k}{(2\pi)^4} V(P,k,q)\chi_P(k), \tag{1}$$

where p_1 represents the quark's momentum, p_2 is the antiquark's momentum; m_1 and m_2 are the masses of the quark and antiquark, respectively, $\chi_P(q)$ denotes the BS wave function of the meson, $V(P,k,q)$ represents the integral kernel of the BS equation, P is the meson's total momentum, and q is the relative momentum between the quark and antiquark. We have the following relation:

$$p_1 = \alpha_1 P + q, \qquad \alpha_1 = \frac{m_1}{m_1+m_2},$$
$$p_2 = \alpha_2 P - q, \qquad \alpha_2 = \frac{m_2}{m_1+m_2}.$$

The BS equation is a four-dimensional integral equation, which is very difficult to solve. So various approximations have been developed to solve it. Among them, the instantaneous approximation is the most frequently used one, which was first proposed by Salpeter and is suitable for heavy mesons. In the center-of-mass system, with the condition of instantaneous approximation, the interaction kernel is simplified as

$$V(P,k,q) \sim V(\vec{k},\vec{q}) = V(\vec{q}-\vec{k}), \tag{2}$$

then the four-dimensional BS equation can be reduced to the three-dimensional Salpeter equation. For simplicity, two functions,

$$\varphi_P(\vec{q}) \equiv i\int \frac{dq_0}{2\pi}\chi_P(q), \tag{3}$$

$$\eta_P(\vec{q}) \equiv \int \frac{d\vec{k}}{(2\pi)^3} V(\vec{k},\vec{q})\varphi_P(\vec{k}), \tag{4}$$

are defined. Thus, the BS equation can be rewritten as

$$\chi_P(q) = S_1(p_1)\eta_P(\vec{q})S_2(-p_2), \tag{5}$$

where $S_1(p_1)$ and $S_2(-p_2)$ are the propagators of the quark 1 and antiquark 2, respectively.

For convenience, we write the formulas in covariant form. Therefore, we divide the relative momentum q into two parts, $q_\parallel$ and $q_\perp$,

$$q_\parallel \equiv \frac{P\cdot q}{M^2}P, \qquad q_\perp \equiv q - q_\parallel,$$

which are parallel and orthogonal to P, respectively, where M is the mass of the relevant meson. Correspondingly, we have two Lorentz-invariant variables,

$$q_P \equiv \frac{P\cdot q}{M}, \qquad q_T \equiv \sqrt{-q_\perp^2},$$

which are q_0 and $|\vec{q}|$ respectively in the center-of-mass system. The propagator S_i ($i = 1, 2$) can be decomposed as

$$S_i = \frac{\Lambda^+_{iP}(q_\perp)}{J(i)q_P + \alpha_i M - \omega_i + i\epsilon} + \frac{\Lambda^-_{iP}(q_\perp)}{J(i)q_P + \alpha_i M + \omega_i - i\epsilon}, \tag{6}$$

where $J(i) = (-1)^{i+1}$, $\omega_i = \sqrt{m_i^2 + q_T^2}$, and

$$\Lambda^\pm_{iP}(q_\perp) = \frac{1}{2\omega_i}\left[\frac{\not{P}}{M}\omega_i \pm J(i)(m_i + \not{q}_\perp)\right].$$

The positive and negative energy projection operators Λ^+ and Λ^- satisfy the following relations:

$$\Lambda^+_{iP}(q_\perp) + \Lambda^-_{iP}(q_\perp) = \frac{\not{P}}{M},$$
$$\Lambda^\pm_{iP}(q_\perp)\frac{\not{P}}{M}\Lambda^\pm_{iP}(q_\perp) = \Lambda^\pm_{iP}(q_\perp),$$
$$\Lambda^\pm_{iP}(q_\perp)\frac{\not{P}}{M}\Lambda^\mp_{iP}(q_\perp) = 0.$$

Introducing the notation,

$$\varphi_P^{\pm\pm}(q_\perp) \equiv \Lambda^\pm_{1P}(q_\perp)\frac{\not{P}}{M}\varphi_P(q_\perp)\frac{\not{P}}{M}\Lambda^\pm_{2P}(q_\perp), \tag{7}$$

and using the relation $\frac{\not{P}}{M}\frac{\not{P}}{M} = 1$, we have

$$\varphi_P(q_\perp) = \varphi_P^{++}(q_\perp) + \varphi_P^{+-}(q_\perp) + \varphi_P^{-+}(q_\perp) + \varphi_P^{--}(q_\perp). \tag{8}$$

Further integrating out q_0 on both sides of Eq. (5), we obtain the Salpeter equation,

$$\varphi_P(q_\perp) = \frac{\Lambda^+_{1P}(q_\perp)\eta_P(q_\perp)\Lambda^+_{2P}(q_\perp)}{M - \omega_1 - \omega_2} - \frac{\Lambda^-_{1P}(q_\perp)\eta_P(q_\perp)\Lambda^-_{2P}(q_\perp)}{M + \omega_1 + \omega_2}. \tag{9}$$

By using the projection operators, this expression can be equivalently written as

$$(M - \omega_1 - \omega_2)\varphi_P^{++}(q_\perp) = \Lambda^+_{1P}(q_\perp)\eta_P(q_\perp)\Lambda^+_{2P}(q_\perp),$$
$$(M + \omega_1 + \omega_2)\varphi_P^{--}(q_\perp) = -\Lambda^-_{1P}(q_\perp)\eta_P(q_\perp)\Lambda^-_{2P}(q_\perp),$$
$$\varphi_P^{+-}(q_\perp) = \varphi_P^{-+}(q_\perp) = 0. \tag{10}$$

The normalization condition for the Salpeter wave function is given by

$$\int \frac{d\vec{q}}{(2\pi)^3}\mathrm{tr}\left[\bar{\varphi}_P^{++}(q_\perp)\frac{\not{P}}{M}\varphi_P^{++}(q_\perp)\frac{\not{P}}{M} - \bar{\varphi}_P^{--}(q_\perp)\frac{\not{P}}{M}\varphi_P^{--}(q_\perp)\frac{\not{P}}{M}\right] = 2M, \tag{11}$$

where, $\bar{\varphi} = \gamma_0\varphi^\dagger\gamma^0$, "†" is the Hermitian conjugate transformation. The relativistic BS equation is four-dimensional, but the Salpeter equation obtained through instantaneous approximation is three-dimensional. Therefore, strictly speaking, the Salpeter equation and the wave function obtained from it are semirelativistic, not completely relativistic.

In our previous works, the complete Salpeter equations for the pseudoscalar [26] and tensor [27] mesons have been solved. The Cornell potential is chosen as the interaction kernel,

$$V(r) = \lambda r + V_0 - \gamma_0 \otimes \gamma^0 \frac{4}{3}\frac{\alpha_s(r)}{r},$$

where λ is the string constant (for heavy-light mesons, $\lambda = 0.25\ \mathrm{GeV}^2$), $\alpha_s(r)$ is the running coupling constant, and V_0 is a free constant. The interaction potential in momentum space is given by

$$V(\vec{q}) = V_s(\vec{q}) + \gamma_0 \otimes \gamma^0 V_v(\vec{q}), \tag{12}$$

$$V_s(\vec{q}) = -\left(\frac{\lambda}{\alpha} + V_0\right)\delta^3(\vec{q}) + \frac{\lambda}{\pi^2}\frac{1}{(\vec{q}^2 + \alpha^2)^2}, \tag{13}$$

$$V_v(\vec{q}) = -\frac{2}{3\pi^2}\frac{\alpha_s(\vec{q})}{(\vec{q}^2 + \alpha^2)}, \tag{14}$$

where

$$\alpha_s(\vec{q}) = \frac{12\pi}{27}\frac{1}{\log\left(a + \frac{\vec{q}^2}{\Lambda^2_{\mathrm{QCD}}}\right)},$$

$a = 2.7183$ and $\Lambda_{\mathrm{QCD}} = 0.27$ GeV. In order to avoid infrared divergence and incorporate the screening effect, a small parameter $\alpha = 0.06$ GeV is added in the potential.

III. WAVE FUNCTIONS AND THEIR PARTIAL WAVES

A. 0^- meson

Usually, people do not solve the complete Salpeter equation, namely the four equations of Eq. (10), but only solves the first one, which is about the positive energy wave function. Due to the fact that $(M + \omega_1 + \omega_2) \gg (M - \omega_1 - \omega_2)$, we have $\varphi_P^{++}(q_\perp) \gg \varphi_P^{--}(q_\perp)$, and $\varphi_P^{--}(q_\perp)$ is negligible. However, this approach also ignored most of the relativistic corrections, because one equation can only solve the case with only one unknown radial wave function. For example, the wave function,

$$\varphi_P(q_\perp) = \left(\frac{\not{P}}{M} + 1\right)\gamma^5 f(q_\perp), \tag{15}$$

is for a pseudoscalar, where the radial wave function $f(q_\perp) \equiv f(-q_\perp^2)$ can be obtained numerically by solving the first equation in Eq. (10). Due to the absence of standalone $q_\perp$ terms, this solving "the incomplete Salpeter equation" method can only obtain nonrelativistic wave function rather than a relativistic one. The correct and safe way is to first solve the complete Salpeter equation and obtain the positive and negative energy wave functions, and then omit the contribution of the negative energy wave function in specific applications.

The Salpeter wave function for a 0^- state has the general form [26],

$$\varphi_{0^-}(q_\perp) = \left[\frac{\not{P}}{M} f_1(q_\perp) + f_2(q_\perp) + \frac{\not{q}_\perp}{M} f_3(q_\perp) + \frac{\not{P}\not{q}_\perp}{M^2} f_4(q_\perp)\right]\gamma^5. \tag{16}$$

We have four unknown radial wave functions $f_i's$, which are function of $-q_\perp^2$. Compared with the nonrelativistic wave function in Eq. (15), our Salpeter wave function has two additional relativistic terms, namely f_3 and f_4 terms, and $f_1 \neq f_2$. So it contains rich relativistic information. Using the last two equations of Salpeter Eq. (10), we get

$$f_3(q_\perp) = \frac{f_2 M(\omega_2 - \omega_1)}{m_2\omega_1 + m_1\omega_2},$$
$$f_4(q_\perp) = -\frac{f_1 M(\omega_1 + \omega_2)}{m_2\omega_1 + m_1\omega_2}.$$

By using the first two equations of the Salpeter Eq. (10), the two unknown independent radial wave functions f_1 an f_2 will be obtained. We do not give the detailed calculation for the 0^- state here. Instead, we will provide the detailed calculation for the more complex 2^+ state in the next subsection. The normalization condition Eq. (11) for this 0^- wave function is [26]

$$\int \frac{d\vec{q}}{(2\pi)^3} \frac{8M\omega_1\omega_2 f_1 f_2}{\omega_1 m_2 + \omega_2 m_1} = 1. \tag{17}$$

We have pointed out that the wave function of the 0^- state not only contains S-wave, namely the terms with f_1 and f_2, but also P-wave components, namely f_3 and f_4 terms [30]. If we only consider the contribution of S-wave, the normalization formula Eq. (17) is

$$\int \frac{d\vec{q}}{(2\pi)^3} \frac{2M f_1 f_2(\omega_1 m_2 + \omega_2 m_1)}{\omega_1\omega_2}. \tag{18}$$

Based on Eqs. (17) and (18), which are $(S+P)^2$ and S^2, the ratio of S-partial wave and P-wave can be calculated [30].

For the 0^- meson, its positive energy-wave function, Eq. (7), can be expressed as

$$\varphi_{0^-}^{++}(q_\perp) = \left[A_1(q_\perp) + \frac{\not{P}}{M} A_2(q_\perp) + \frac{\not{q}_\perp}{M} A_3(q_\perp) + \frac{\not{P}\not{q}_\perp}{M^2} A_4(q_\perp)\right]\gamma^5, \tag{19}$$

where A_1 and A_2 terms are S-waves, and A_3 and A_4 terms are P-waves. Their detailed expressions are as follows:

$$A_1 = \frac{M}{2}\left(\frac{f_1(\omega_1+\omega_2)}{m_1+m_2} + f_2\right), \qquad A_3 = -\frac{A_1 M(\omega_1-\omega_2)}{m_2\omega_1 + m_1\omega_2},$$
$$A_2 = \frac{M}{2}\left(\frac{f_2(m_1+m_2)}{\omega_1+\omega_2} + f_1\right), \qquad A_4 = -\frac{A_1 M(m_1+m_2)}{m_2\omega_1 + m_1\omega_2}.$$

B. 2^+ meson

The bound state with quantum number $J^P = 2^+$ can be described by the following Salpeter wave function [27]:

$$\begin{aligned}\varphi_{2^+}(q_\perp) = {}& \epsilon_{\mu\nu} q_\perp^\mu q_\perp^\nu \left[\zeta_1(q_\perp) + \frac{\not{P}}{M}\zeta_2(q_\perp) + \frac{\not{q}_\perp}{M}\zeta_3(q_\perp) + \frac{\not{P}\not{q}_\perp}{M^2}\zeta_4(q_\perp)\right] \\ & + M\epsilon_{\mu\nu}\gamma^\mu q_\perp^\nu \left[\zeta_5(q_\perp) + \frac{\not{P}}{M}\zeta_6(q_\perp) + \frac{\not{q}_\perp}{M}\zeta_7(q_\perp) + \frac{\not{P}\not{q}_\perp}{M^2}\zeta_8(q_\perp)\right],\end{aligned} \tag{20}$$

where $\varepsilon_{\mu\nu}$ is the symmetric polarization tensor of the meson; the unknown radial wave function $\zeta_i(q_\perp)$ $(i = 1, 2\ldots 8)$ is function of $-q_\perp^2$, which will be obtained by solving the Salpeter equation. Using the last two equations of Eq. (10), it is found that only four radial wave functions are independent. We choose $\zeta_3(q_\perp)$, $\zeta_4(q_\perp)$, $\zeta_5(q_\perp)$, and $\zeta_6(q_\perp)$ as the independent ones, and others can be expressed as

$$\zeta_1(q_\perp) = \frac{q_\perp^2\zeta_3(\omega_1+\omega_2) + 2\zeta_5 M^2\omega_2}{M(m_2\omega_1 + m_1\omega_2)},$$
$$\zeta_7(q_\perp) = \frac{M(\omega_1-\omega_2)}{m_2\omega_1 + m_1\omega_2}\zeta_5,$$
$$\zeta_2(q_\perp) = \frac{q_\perp^2\zeta_4(\omega_1-\omega_2) + 2\zeta_6 M^2\omega_2}{M(m_2\omega_1 + m_1\omega_2)},$$
$$\zeta_8(q_\perp) = \frac{M(\omega_1+\omega_2)}{m_2\omega_1 + m_1\omega_2}\zeta_6.$$

From Eq. (7), we obtain the expressions of positive and negative energy wave functions. For example, the positive energy-wave function of 2^+ meson is

$$\varphi_{2^+}^{++}(q_\perp) = \epsilon_{\mu\nu} q_\perp^\mu q_\perp^\nu \left[B_1(q_\perp) + \frac{\not P}{M} B_2(q_\perp) + \frac{\not q_\perp}{M} B_3(q_\perp) + \frac{\not P \not q_\perp}{M^2} B_4(q_\perp)\right]$$
$$+ M\epsilon_{\mu\nu}\gamma^\mu q_\perp^\nu \left[B_5(q_\perp) + \frac{\not P}{M} B_6(q_\perp) + \frac{\not q_\perp}{M} B_7(q_\perp) + \frac{\not P \not q_\perp}{M^2} B_8(q_\perp)\right], \tag{21}$$

where B_is are functions of four independent radial wave functions ζ_3, ζ_4, ζ_5, and ζ_6. Their specific expression are denoted as

$$B_1 = \frac{1}{2M(m_1\omega_2 + m_2\omega_1)}[(\omega_1+\omega_2)q_\perp^2\zeta_3 + (m_1+m_2)q_\perp^2\zeta_4 + 2M^2\omega_2\zeta_5 - 2M^2 m_2\zeta_6],$$
$$B_2 = \frac{1}{2M(m_1\omega_2 + m_2\omega_1)}[(m_1-m_2)q_\perp^2\zeta_3 + (\omega_1-\omega_2)q_\perp^2\zeta_4 + 2M^2\omega_2\zeta_6 - 2M^2 m_2\zeta_5],$$
$$B_3 = \frac{1}{2}\left[\zeta_3 + \frac{m_1+m_2}{\omega_1+\omega_2}\zeta_4 - \frac{2M^2}{m_1\omega_2+m_2\omega_1}\zeta_6\right], \qquad B_5 = \frac{1}{2}\left[\zeta_5 - \frac{\omega_1+\omega_2}{m_1+m_2}\zeta_6\right],$$
$$B_4 = \frac{1}{2}\left[\frac{\omega_1+\omega_2}{m_1+m_2}\zeta_3 + \zeta_4 - \frac{2M^2}{m_1\omega_2+m_2\omega_1}\zeta_5\right], \qquad B_6 = \frac{1}{2}\left[-\frac{m_1+m_2}{\omega_1+\omega_2}\zeta_5 + \zeta_6\right],$$
$$B_7 = \frac{M}{2}\frac{\omega_1-\omega_2}{m_1\omega_2+m_2\omega_1}\left[\zeta_5 - \frac{\omega_1+\omega_2}{m_1+m_2}\zeta_6\right], \qquad B_8 = \frac{M}{2}\frac{m_1+m_2}{m_1\omega_2+m_2\omega_1}\left[-\zeta_5 + \frac{\omega_1+\omega_2}{m_1+m_2}\zeta_6\right].$$

Substituting the positive and negative wave functions into the first two equations of Eq. (10), and multiplying both sides by the same variable (for example, $\not P$, $\not q_\perp$, $\not q_\perp \not P$, etc.), we calculate the trace on both sides, and find there are four (not two) independent eigenvalue equations. For convenience, we have replaced $\zeta_3(q_\perp)$, $\zeta_4(q_\perp)$, $\zeta_5(q_\perp)$, and $\zeta_6(q_\perp)$, with $F_1(q_\perp)$, $F_2(q_\perp)$, $F_3(q_\perp)$, and $F_4(q_\perp)$. Their relations are

$$F_1(q_\perp) = \frac{4q_\perp^4[(\omega_1+\omega_2)(\zeta_5 M^2 + \zeta_3 q_\perp^2) - (m_1+m_2)(\zeta_6 M^2 - \zeta_4 q_\perp^2)]}{3M(m_2\omega_1 + m_1\omega_2)}, \tag{22}$$

$$F_2(q_\perp) = \frac{4q_\perp^4[(m_1+m_2)(\zeta_6 M^2 - \zeta_4 q_\perp^2) + (\omega_1+\omega_2)(\zeta_5 M^2 + \zeta_3 q_\perp^2)]}{3M(m_2\omega_1 + m_1\omega_2)}, \tag{23}$$

$$F_3(q_\perp) = \frac{2q_\perp^4[-\zeta_5(5m_1+m_2)M^2 - 2(\zeta_3(m_1-m_2)q_\perp^2 + \zeta_4 q_\perp^2(\omega_1-\omega_2)) + \zeta_6 M^2(5\omega_1+\omega_2)]}{3M(m_2\omega_1 + m_1\omega_2)}, \tag{24}$$

$$F_4(q_\perp) = \frac{2q_\perp^4[\zeta_5(5m_1+m_2)M^2 - 2(\zeta_4 q_\perp^2(\omega_1-\omega_2) - \zeta_3(m_1-m_2)q_\perp^2) + \zeta_6 M^2(5\omega_1+\omega_2)]}{3M(m_2\omega_1 + m_1\omega_2)}. \tag{25}$$

The obtained four coupled eigenvalue equations are presented in the Appendix.

The normalization condition Eq. (11) for the 2^+ wave function is [27]

$$\int \frac{d\vec{q}}{(2\pi)^3}\frac{8M\omega_1\omega_2\vec{q}^2}{15(\omega_1 m_2 + \omega_2 m_1)}\left[-\zeta_5\zeta_6 + \frac{2\vec{q}^2}{M^2}\left(-\zeta_4\zeta_5 + \zeta_3\zeta_6 + \zeta_3\zeta_4\frac{\vec{q}^2}{M^2}\right)\right] = 1. \tag{26}$$

In our expression, the 2^+ state $\bar{D}_2^\star(2460)^0$, is not a pure P-wave, but contains both D- and F-partial waves [30]. In Eq. (20), the terms including ζ_5 and ζ_6 are P-waves which are nonrelativistic, ζ_3 and ζ_4 terms are $F-P$ mixing waves, and others are D-waves. Thus, we can conclude that the wave function of the tensor $\bar{D}_2^\star(2460)^0$ contains P-, D-, and F-partial waves.

If only the pure P-wave is considered, the wave function of the 2^+ meson becomes

$$\varphi_{2^+}^{P}(q_\perp) = \epsilon_{\mu\nu} q_\perp^\mu \gamma^\nu (M\zeta_5 + \not P\zeta_6) + \frac{2}{5}\epsilon_{\mu\nu} q_\perp^\mu \gamma^\nu q_\perp^2\left(\frac{\zeta_3}{M} - \frac{\not P}{M^2}\zeta_4\right), \tag{27}$$

and the contribution of this P-partial wave to the overall normalization condition Eq. (26) is

$$\int \frac{d\vec{q}}{(2\pi)^3} \frac{2\vec{q}^2(2\zeta_3\vec{q}^2 - 5\zeta_5 M^2)(2\zeta_4\vec{q}^2 + 5\zeta_6 M^2)(\omega_1 m_2 + \omega_2 m_1)}{75M^3\omega_1\omega_2}. \tag{28}$$

While for a pure F-wave, the wave function is

$$\varphi_{2^+}^F(q_\perp) = \epsilon_{\mu\nu} q_\perp^\mu q_\perp^\nu \left(\frac{\not{q}_\perp}{M}\zeta_3 + \frac{\not{P}\not{q}_\perp}{M^2}\zeta_4\right) - \frac{2}{5}\epsilon_{\mu\nu} q_\perp^\mu \gamma^\nu q_\perp^2 \left(\frac{\zeta_3}{M} - \frac{\not{P}}{M^2}\zeta_4\right), \tag{29}$$

and its contribution to the normalization condition Eq. (26) is

$$\int \frac{d\vec{q}}{(2\pi)^3} \frac{4\zeta_3\zeta_4\vec{q}^6(\omega_1 m_2 + \omega_2 m_1)}{25M^3\omega_1\omega_2}. \tag{30}$$

Using Eqs. (26), (28), and (30), we can calculate the ratios between different partial waves.

IV. SEMILEPTONIC DECAY WIDTH FORMULA

For the $B^+ \to \bar{D}_2^\star(2460)^0\ell^+\nu_\ell$ process as shown in Fig. 1, the transition amplitude is written as

$$T = \frac{G_F}{\sqrt{2}} V_{cb}\bar{\mu}_{\nu_\ell}\gamma^\mu(1-\gamma^5)\upsilon_\ell \langle D_2^\star(2460)^0(P_f)|J_\mu|B^+(P)\rangle, \tag{31}$$

where G_F is the Fermi constant, $J_\mu \equiv V_\mu - A_\mu$ is the charged current responsible for the decays, $V_{cb} = 40.5 \times 10^{-3}$ (PDG [34]) is CKM matrix element, μ_{ν_ℓ} is the spinor of the neutrino ν_ℓ, υ_ℓ is the spinor of the antilepton ℓ^+, P, and P_f are the momenta of the initial B^+ and the final $\bar{D}_2^\star(2460)^0$, respectively.

After summing the polarizations of the initial and final mesons, the square of the above matrix elements is written as

$$\sum |T^2| = \frac{G_F^2}{2}|V_{cb}|^2\ell^{\mu\nu}h_{\mu\nu}, \tag{32}$$

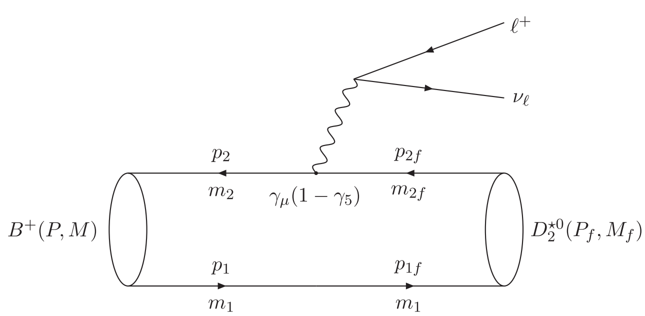

FIG. 1. Feynman diagram corresponding to the semileptonic decay $B^+ \to \bar{D}_2^\star(2460)^0\ell^+\nu_\ell$.

where $\ell^{\mu\nu} \equiv \sum \bar{\mu}_{\nu_\ell}\gamma^\mu(1-\gamma_5)\upsilon_\ell\bar{\upsilon}_\ell(1+\gamma_5)\gamma^\nu\mu_{\nu_\ell}$ is the leptonic tensor, and $h_{\mu\nu} \equiv \sum \langle B^+(P)|J_\nu^+|D_2^\star(2460)^0(P_f)\rangle \times \langle D_2^\star(2460)^0(P_f)|J_\mu|B^+(P)\rangle$ is the hadron tensor.

By using Mandelstam's formulism, the hadronic transition matrix element can be written as the overlapping integral over the BS wave functions of the initial and final mesons. Since we do not solve the BS equation, but the Salpeter equation, the transition matrix element is further simplified by instantaneous approximation. Then, for the process $B^+ \to \bar{D}_2^\star(2460)^0\ell^+\nu_\ell$, the hadronic matrix element can be written as [35]

$$\begin{aligned}
&\langle D_2^\star(2460)^0(P_f)|J_\mu|B^+(P)\rangle \\
&\quad = \int \frac{d\vec{q}}{(2\pi)^3}\mathrm{Tr}\left[\frac{\not{P}}{M}\varphi_P^{++}(\vec{q})\gamma_\mu(1-\gamma_5)\bar{\varphi}_{P_f}^{++}(\vec{q}_f)\right] \\
&\quad = t_1\epsilon_{\mu P} + t_2\epsilon_{PP}P_\mu + t_3\epsilon_{PP}P_{f\mu} + it_4\epsilon^{\rho P}\varepsilon_{\rho PP_f\mu},
\end{aligned} \tag{33}$$

where $\vec{q}_f = \vec{q} - \alpha_{1f}\vec{P}_f$ is used, which is obtained by assuming the momentum of spectator quark remains unchanged; $\epsilon_{\mu\nu}$ is the polarization tensor of the final tensor meson, t_1, t_2, t_3 and t_4 are the form factors, φ_P^{++} and $\bar{\varphi}_{P_f}^{++} = \gamma_0(\varphi_{P_f}^{++})^\dagger\gamma^0$ are the positive energy Salpeter wave functions for the initial and final mesons, respectively. We have used the abbreviations, for example $\epsilon^{\rho\sigma}P_\sigma\varepsilon_{\rho\alpha\beta\mu}P^\alpha P_f{}^\beta = \epsilon^{\rho P}\varepsilon_{\rho PP_f\mu}$.

Based on the covariance analysis of the Lorenz index, the general form of $h_{\mu\nu}$ can be expressed as

$$\begin{aligned}
h_{\mu\nu} = &-\alpha g_{\mu\nu} + \beta_{++}(P+P_f)_\mu(P+P_f)_\nu \\
&+ \beta_{+-}(P+P_f)_\mu(P-P_f)_\nu \\
&+ \beta_{-+}(P-P_f)_\mu(P+P_f)_\nu \\
&+ \beta_{--}(P-P_f)_\mu(P-P_f)_\nu \\
&+ i\gamma\varepsilon_{\mu\nu\rho\sigma}(P+P_f)^\rho(P-P_f)^\sigma,
\end{aligned} \tag{34}$$

where, the coefficients α, $\beta_{\pm\pm}$ and γ are functions of the form factors t_i ($i = 1, 2, 3, 4$). Thus, the differential decay rate of this exclusive process can be written as

$$\frac{d^2\Gamma}{dxdy} = |V_{ij}|^2 \frac{G_F^2 M^5}{32\pi^3} \left\{ \alpha \frac{\left(y - \frac{m_\ell^2}{M^2}\right)}{M^2} + 2\beta_{++} \times \left[2x\left(1 - \frac{M_f^2}{M^2} + y\right) - 4x^2 - y + \frac{m_\ell^2}{4M^2}\left(8x + \frac{4M_f^2 - m_\ell^2}{M^2} - 3y\right)\right] + (\beta_{+-} + \beta_{-+})\frac{m_\ell^2}{M^2}\left(2 - 4x + y - \frac{2M_f^2 - m_\ell^2}{M^2}\right) + \beta_{--}\frac{m_\ell^2}{M^2}\left(y - \frac{m_\ell^2}{M^2}\right) - \gamma\left[y\left(1 - \frac{M_f^2}{M^2} - 4x + y\right) + \frac{m_\ell^2}{M^2}\left(1 - \frac{M_f^2}{M^2} + y\right)\right]\right\}, \tag{35}$$

where $x \equiv E_\ell/M$, $y \equiv (P - P_f)^2/M^2$, M, and M_f are the masses of B^+ and $\bar{D}_2^\star(2460)^0$, respectively, and m_ℓ and E_ℓ are the mass and energy of the final charged lepton ℓ, respectively.

V. RESULTS AND DISCUSSION

In the calculation, we used the constituent quark masses; $m_u = 0.38$ GeV, $m_d = 0.385$ GeV, $m_s = 0.55$ GeV, $m_c = 1.62$ GeV, and $m_b = 4.96$ GeV. Other model-dependent parameters have been shown in the text. In our calculation, for each J^P, the ground-state mass is our input, that is, its value is obtained by fitting experimental data to determine the free parameter V_0. And the masses of excited states are our predictions. Therefore, the masses of B, B_s, and B_c are the same as the experimental values and are not reiterated here. The mass spectra for the tensor 2^{++} states are provided in Table I.

A. The wave functions and ratios of different partial waves

The numerical values of the radial wave functions for 0^- pseudoscalars B and B_s are shown in Fig. 2 (for B_c meson, see Ref. [30]). We can see the S-wave components, namely the f_1 and f_2 terms in Eq. (16), are dominant, and the P-wave ones, namely f_3 and f_4 terms, are small. So, B^+, B^0, B_s^0, and B_c^+ are all S-wave dominant states. To see this clearly, we calculate the ratio between S- and P-waves which are based on the normalization formulas Eqs. (17) and (18), and the results are shown in Table II.

In a nonrelativistic limit, only the S-wave survives, and $f_1 = f_2$ for a 0^- meson. In our semirelativistic method, first, radial wave function f_1 is not exactly equal to f_2, and second, the 0^- wave function also includes the P-wave components, f_3 and f_4 terms, which contribute to the relativistic correction. The ratios in Table II, indicate that the relativistic correction in B^+ (or B^0) is a little larger than that of B_s^0, and much larger than that of B_c^+.

For the 2^+ tensors, in our semirelativistic method, their wave functions contain 8 terms, of which four are independent. The four independent radial wave functions for 2^+ mesons $\bar{D}_2^{\star 0}(nP)$ and $D_{s2}^{\star -}(nP)$ ($n = 1, 2, 3$) are shown in Figs. 3 and 4, respectively.

Among the eight terms of the wave function for a tensor, ζ_5 and ζ_6 terms are P-waves, ζ_3 and ζ_4 terms are mixture of P and F waves, and others, ζ_1, ζ_2, ζ_7, and ζ_8 are D-waves. Figures 3 and 4 roughly show us that the 2^+ wave function is dominated by P wave, which is consistent with the description of a nonrelativistic method, where only a P-wave exists with $\zeta_5 = -\zeta_6$. In order to show the proportion of different waves, we use the normalization formulas, Eqs. (26), (28), and (30), to calculate the their ratios, and the results are shown in Table III. We can see that, the P-wave is dominant, the D-wave is also sizable, and the F-wave is very small.

In the nonrelativistic limit, only P-wave exists, our results confirm that the P-wave is dominant, so these states are marked as $1P$, $2P$, and $3P$ states in Figs. 3 and 4, and in Tables I and III, respectively. Compared with the nonrelativistic P-waves from ζ_5 and ζ_6 terms, the D- and F-waves, as well as the P-waves from ζ_3 and ζ_4 terms in the 2^+ wave function provide the relativistic correction. From Table III, it can be seen that for the $1P$, $2P$, and $3P$ states, the proportion of F-wave is very small and can be ignored when precise calculation is not required. Based on the proportions of D-wave in Table III, we conclude that, the relativistic correction in $D_2^\star$ is a little larger than that of $D_{s2}^\star$, and much larger than that in χ_{c2}. It also shows that the relativistic correction of the highly excited state is larger than that of the lowly excited one, and the latter is larger than that of the ground state.

TABLE I. Mass spectra of the 2^+ tensors in unit of GeV.

	$m_{\bar{D}_2^{\star 0}}$	$m_{D_2^{\star -}}$	$m_{D_{s2}^{\star -}}$	$m_{\chi_{c2}}$
$1\,^3P_2$	2.461 (input)	2.465 (input)	2.569 (input)	3.556 (input)
$2\,^3P_2$	2.985	2.992	3.111	3.972
$3\,^3P_2$	3.342	3.352	3.474	4.270

B. The branching ratios of the semileptonic decays

With the numerical values of wave functions and the formula for the transition matrix element, Eq. (33), the

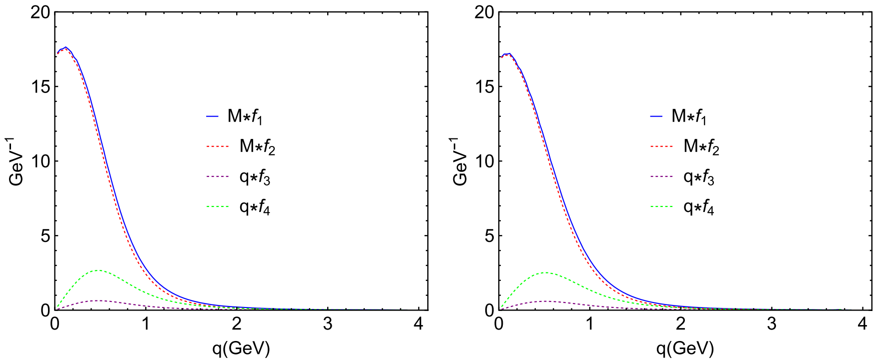

FIG. 2. The radial wave functions of the 0^- mesons B^+ (left) and B_s^0 (right), where f_1 and f_2 terms are S-waves; f_3 and f_4 terms are P-waves, and $q \equiv |\vec{q}|$.

calculation of the semileptonic decay is straightforward. We present our results for branching ratios and other theoretical predictions in Table IV. It is observed that there are few theoretical results in the literature regarding the case of highly excited tensor particles as the final state. Almost all existing results focus on studying the $1P$ final-state process, with significant differences in predictions from different models, especially for $B^+ \to \bar{D}_2^{\star 0}(1P)\ell\nu_\ell$, whose branching ratios vary from 1.01 to 38.0.

Currently, only the production of the ground state $D_2^\star(1P)$ in the semileptonic decay of the B meson and its cascade strong decay have been detected in experiments. The decay chains are $B \to D_2^\star(2460)\ell\nu_\ell$, $D_2^\star(2460) \to D\pi$. The averaged experimental results are [34]

$$\begin{aligned}
&\mathcal{B}(B^+ \to \bar{D}_2^{\star 0}\ell^+\nu_\ell)\mathcal{B}(\bar{D}_2^{\star 0} \to D^-\pi^+) \\
&\quad = (1.53 \pm 0.16) \times 10^{-3}, \\
&\mathcal{B}(B^+ \to \bar{D}_2^{\star 0}\ell^+\nu_\ell)\mathcal{B}(\bar{D}_2^{\star 0} \to D^{\star -}\pi^+) \\
&\quad = (1.01 \pm 0.24) \times 10^{-3},
\end{aligned} \tag{36}$$

$$\begin{aligned}
&\mathcal{B}(B^0 \to D_2^{\star -}\ell^+\nu_\ell)\mathcal{B}(D_2^{\star -} \to \bar{D}^0\pi^-) \\
&\quad = (1.21 \pm 0.33) \times 10^{-3}, \\
&\mathcal{B}(B^0 \to D_2^{\star -}\ell^+\nu_\ell)\mathcal{B}(D_2^{\star -} \to \bar{D}^{\star 0}\pi^-) \\
&\quad = (0.68 \pm 0.12) \times 10^{-3}.
\end{aligned} \tag{37}$$

The mass of $D_2^\star$ is above the thresholds of $D\pi$ and $D^\star\pi$, so $D_2^\star$ has the OkuboZweigIizuka-allowed strong decay channels $D_2^\star \to D\pi$ and $D_2^\star \to D^\star\pi$, which are the dominant decay processes of $D_2^\star$. Reference [52] predicted $\mathcal{B}(\bar{D}_2^{\star 0} \to D^-\pi^+) = \mathcal{B}(D_2^{\star -} \to \bar{D}^0\pi^-) = 44.5\%$ and $\mathcal{B}(\bar{D}_2^{\star 0} \to D^{\star -}\pi^+) = \mathcal{B}(D_2^{\star -} \to \bar{D}^{\star 0}\pi^-) = 21.0\%$. Using these, our theoretical predictions are

$$\begin{aligned}
&\mathcal{B}(B^+ \to \bar{D}_2^{\star 0}\ell^+\nu_\ell)\mathcal{B}(\bar{D}_2^{\star 0} \to D^-\pi^+) = 1.33 \times 10^{-3}, \\
&\mathcal{B}(B^+ \to \bar{D}_2^{\star 0}\ell^+\nu_\ell)\mathcal{B}(\bar{D}_2^{\star 0} \to D^{\star -}\pi^+) = 0.628 \times 10^{-3},
\end{aligned} \tag{38}$$

$$\begin{aligned}
&\mathcal{B}(B^0 \to D_2^{\star -}\ell^+\nu_\ell)\mathcal{B}(D_2^{\star -} \to \bar{D}^0\pi^-) = 1.23 \times 10^{-3}, \\
&\mathcal{B}(B^0 \to D_2^{\star -}\ell^+\nu_\ell)\mathcal{B}(D_2^{\star -} \to \bar{D}^{\star 0}\pi^-) = 0.582 \times 10^{-3}.
\end{aligned} \tag{39}$$

The first two are slightly smaller than the experimental values, while the last two are in good agreement with the experimental data.

Similarly, using $\mathcal{B}(D_{s2}^{\star -} \to \bar{D}^0K^-) = 48.7\%$ and $\mathcal{B}(D_{s2}^{\star -} \to D^-\bar{K}^0) = 44.1\%$ from Ref. [52], we obtain

$$\begin{aligned}
&\mathcal{B}(B_s^0 \to D_{s2}^{\star -}\ell^+\nu_\ell)\mathcal{B}(D_{s2}^{\star -} \to \bar{D}^0K^-) = 1.83 \times 10^{-3}, \\
&\mathcal{B}(B_s^0 \to D_{s2}^{\star -}\ell^+\nu_\ell)\mathcal{B}(D_{s2}^{\star -} \to D^-\bar{K}^0) = 1.66 \times 10^{-3}.
\end{aligned} \tag{40}$$

Compared to the ground $1P$ final-state case, our results show that the branching ratio of the process with a highly excited final state ($2P$ or $3P$) is very small. The small branching ratio may be caused by the node structures (see Figs. 3 and 4) in the wave functions of the excited $2P$ and $3P$ mesons. The contributions of the wave functions on both sides of the node cancel each other, resulting in a very small branching ratio.

In Table IV, the ratios $\mathcal{R}(\bar{D}_2^{\star 0})$, $\mathcal{R}(D_2^{\star -})$, $\mathcal{R}(D_{s2}^\star)$, and $\mathcal{R}(\chi_{c2})$ are also listed, where, for example,

$$\mathcal{R}(\bar{D}_2^{\star 0}) = \frac{\mathcal{B}(B^+ \to \bar{D}_2^{\star 0}(1P)\tau\nu_\tau)}{\mathcal{B}(B^+ \to \bar{D}_2^{\star 0}(1P)\ell\nu_\ell)}. \tag{41}$$

The ratio $\mathcal{R}$ may cancel some model-dependent factors, which can be seen from the results of Refs. [37,39], and ours. The branching ratios are much different, but the $\mathcal{R}(\bar{D}_2^{\star 0})$ values is around 0.04, which is very close to each other. We have similar conclusions for $\mathcal{R}(D_{s2}^\star)$ and $\mathcal{R}(\chi_{c2})$.

TABLE II. Ratios between the S wave and P wave in the 0^- wave function.

0^- meson	B^+	B^0	B_s^0	B_c^+
$S:P$	1:0.339	1:0.333	1:0.227	1:0.0815

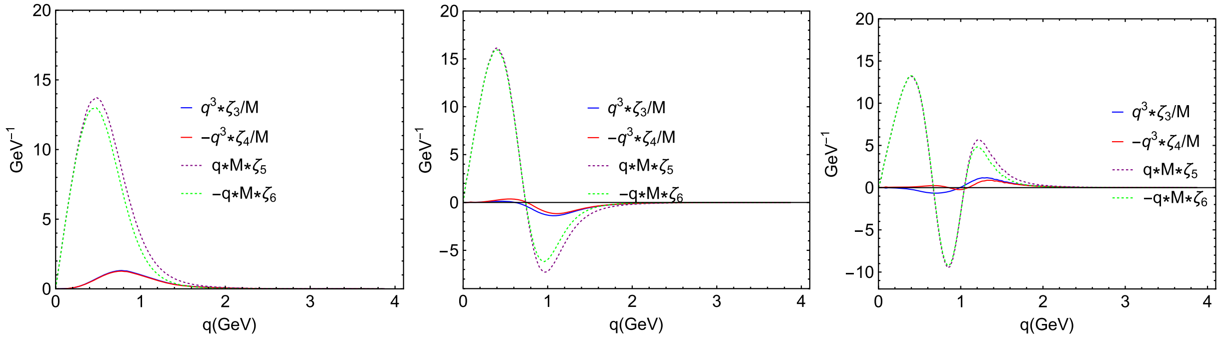

FIG. 3. The four independent radial wave functions for the 2^+ tensors $\bar{D}_2^{\star 0}(1P)$ (left), $\bar{D}_2^{\star 0}(2P)$ (middle) and the $\bar{D}_2^{\star 0}(3P)$ (right).

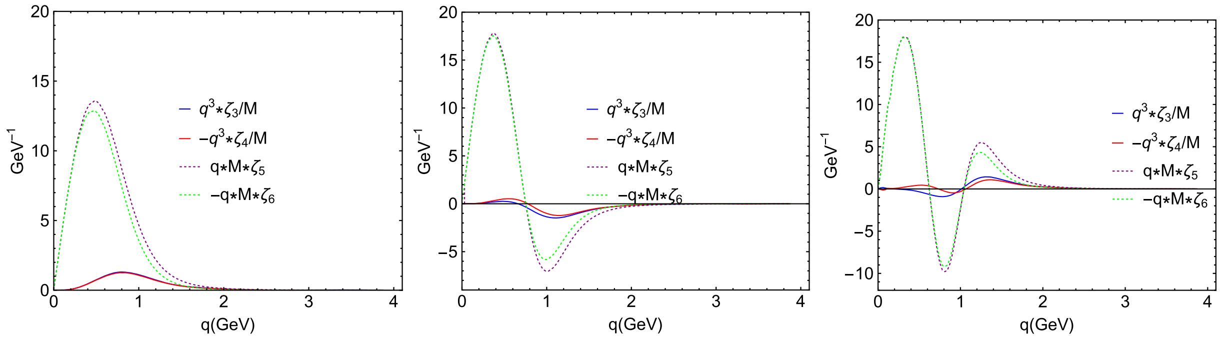

FIG. 4. The four independent radial wave functions for the 2^+ tensors $D_{s2}^{\star -}(1P)$ (left), $D_{s2}^{\star -}(2P)$ (middle) and the $D_{s2}^{\star -}(3P)$ (right).

We have pointed out that the relativistic corrections of excited states are greater than those of ground states [23,30]. And there are still significant differences in semileptonic decays between theoretical results, especially for the B decays. The differences may be caused by the relativistic corrections. So for these processes, which contains excited states, we need a more careful study, especially the relativistic corrections. In the following, we will study the detailed contributions of different partial waves.

C. Contributions of different partial waves

We provide the proportions of different partial waves in the wave function, allowing us to roughly estimate the magnitude of the relativistic correction. However, this does not represent the true relativistic correction of particles in interaction, as different partial waves behave differently in interactions. What we need is the overlapping integration between wave functions, not the individual wave functions themselves. Therefore, using some transition processes as examples, we present the detailed contributions of partial waves.

TABLE III. Ratios between the partial waves in the 2^+ wave function.

2^+		$1P$	$2P$	$3P$
$D_2^{\star 0}$	$P{:}D{:}F$	1:0.393:0.0729	1:0.461:0.0787	1:0.560:0.0640
$D_2^{\star -}$	$P{:}D{:}F$	1:0.389:0.0732	1:0.456:0.0793	1:0.550:0.0657
$D_{s2}^{\star -}$	$P{:}D{:}F$	1:0.298:0.0743	1:0.349:0.0843	1:0.404:0.0813
χ_{c2}	$P{:}D{:}F$	1:0.140:0.0551	1:0.160:0.0673	1:0.177:0.0726

1. $B^+ \to \bar{D}_2^{\star 0}(1P)\ell^+\nu_\ell$

Table II shows that the wave function of B^+ is dominated by S-waves (A_1 and A_2 terms) but mixed with P-waves (A_3 and A_4 terms), their ratio is $S{:}P = 1{:}0.339$. For $\bar{D}_2^{\star 0}$, P-wave is dominant and mixed with D- and F-waves, $P{:}D{:}F = 1{:}0.393{:}0.0729$.

To see the detail of the transition $B^+ \to \bar{D}_2^{\star 0}(1P)$, we will carefully study the overlapping integral of $(S+P)\times(P'+D'+F')$, where to distinguish between the initial and final states, we use "prime" to represent the final state. We show some of the detailed contributions of different partial waves to the branching ratio of $B^+ \to \bar{D}_2^{\star 0}(1P)\ell^+\nu_\ell$ in Table V. Where "whole" means the complete wave function, while "S-wave" in the column or "P'-wave" in the row means the corresponding result is obtained only using the S- or P'-wave and ignoring others, etc.

From Table V, we can see that the dominant S-partial wave in the B^+ state and P'-wave in $\bar{D}_2^{\star 0}(1P)$ provide the dominant contribution. The P-wave in B^+ and D'-wave in $\bar{D}_2^{\star 0}(1P)$ give the main relativistic corrections, while the F'-partial wave in $\bar{D}_2^{\star 0}(1P)$ has a tiny contribution, which can be safely ignored.

TABLE IV. Branching ratios (10^{-3}) of semileptonic decays and ratios $\mathcal{R}(D_2^\star)$, $\mathcal{R}(D_{s2}^\star)$, and $\mathcal{R}(\chi_{c2})$.

Process						Ours
$B^+ \to \bar{D}_2^{\star 0}(1P)\ell\nu_\ell$	4.5~8.0 [36]	38.0 [37]	1.01 [38]	12.3 [39]a	6.3 [39]b	2.99
$B^+ \to \bar{D}_2^{\star 0}(1P)\tau\nu_\tau$		1.5 [37]	0.16 [38]	0.49 [39]a	0.22 [39]b	0.135
$\frac{\mathcal{B}(B^+ \to \bar{D}_2^{\star 0}(1P)\tau\nu_\tau)}{\mathcal{B}(B^+ \to \bar{D}_2^{\star 0}(1P)\ell\nu_\ell)}$		0.041 [37]	0.16 [38]	0.040 [39]a	0.035 [39]b	0.045
$B^+ \to \bar{D}_2^{\star 0}(2P)\ell\nu_\ell$						0.075
$B^+ \to \bar{D}_2^{\star 0}(3P)\ell\nu_\ell$						0.0024
$B^0 \to D_2^{\star -}(1P)\ell\nu_\ell$	3.1(3.8) [40]	2.5 [41]	5.9 [42]	5.86 [43]		2.77
$B^0 \to D_2^{\star -}(1P)\tau\nu_\tau$						0.125
$\frac{\mathcal{B}(B^0 \to D_2^{\star -}(1P)\tau\nu_\tau)}{\mathcal{B}(B^0 \to D_2^{\star -}(1P)\ell\nu_\ell)}$						0.045
$B^0 \to D_2^{\star -}(2P)\ell\nu_\ell$						0.070
$B^0 \to D_2^{\star -}(3P)\ell\nu_\ell$						0.0022
$B_s^0 \to D_{s2}^{\star -}(1P)\ell\nu_\ell$	3.5 [41]	4.32 [44]	2.2 [45]	6.7 [46]	3.76 [47]	3.76
$B_s^0 \to D_{s2}^{\star -}(1P)\tau\nu_\tau$		0.31 [44]	0.926 [45]	0.29 [46]		0.182
$\frac{\mathcal{B}(B_s^0 \to D_{s2}^{\star -}(1P)\tau\nu_\tau)}{\mathcal{B}(B_s^0 \to D_{s2}^{\star -}(1P)\ell\nu_\ell)}$		0.071 [44]	0.42 [45]	0.043 [46]		0.048
$B_s^0 \to D_{s2}^{\star -}(2P)\ell\nu_\ell$						0.124
$B_s^0 \to D_{s2}^{\star -}(3P)\ell\nu_\ell$						0.0047
$B_c^+ \to \chi_{c2}(1P)\ell\nu_\ell$	1.0 [41]	1.6 [48]	1.7 [49]	1.3 [50]	2.12 [51]	1.82
$B_c^+ \to \chi_{c2}(1P)\tau\nu_\tau$		0.093 [48]	0.082 [49]	0.093 [50]	0.33 [51]	0.108
$\frac{\mathcal{B}(B_c^+ \to \chi_{c2}(1P)\tau\nu_\tau)}{\mathcal{B}(B_c^+ \to \chi_{c2}(1P)\ell\nu_\ell)}$		0.058 [48]	0.048 [49]	0.072 [50]	0.15 [51]	0.059
$B_c^+ \to \chi_{c2}(2P)\ell\nu_\ell$		0.033 [48]				0.187
$B_c^+ \to \chi_{c2}(3P)\ell\nu_\ell$						0.0271

For the B^+ meson, its nonrelativistic wave function only contains S-wave, so its P-wave provides the relativistic correction. For the $D_2^{\star 0}(1P)$, the situation is relatively complex. In the nonrelativistic case, its wave function only contains P'-waves, but only P'-waves from ζ_5 and ζ_6 terms, without the ones from ζ_3 and ζ_4 terms, see the formula in Eq. (33). Therefore, in the nonrelativistic scenario, the branching ratio of $S \times P'$ changes from 35.6×10^{-4} in Table V to 37.2×10^{-4}. Our complete branching ratio is $\mathcal{B}_{\rm rel} = 29.9 \times 10^{-4}$, so the relativistic effect can be calculated as

$$\frac{\mathcal{B}_{\text{non-rel}} - \mathcal{B}_{\rm rel}}{\mathcal{B}_{\rm rel}} = 24.4\%, \tag{42}$$

which is significant but not as large as expected. This might be due to two possible reasons. First, there could be a cancellation between relativistic corrections; for example, the contribution of overlapping $P \times P'$ is 4.45×10^{-4}, $P \times D'$ is 10.1×10^{-4}, while their sum contribution $P \times (P' + D')$ is 1.48×10^{-4}. Second, from Table V, we can see that the main relativistic correction is from the interaction $P \times D'$, not from $S \times D'$ or $P \times P'$.

2. $B^+ \to \bar{D}_2^{\star 0}(2P)\ell^+\nu_\ell$

Table VI shows the details of the decay $B^+ \to \bar{D}_2^{\star 0}(2P)\ell^+\nu_\ell$. Compared with the case of $\bar{D}_2^{\star 0}(1P)$ final state, the contributions of all the partial waves are much smaller. The main reason is that there are nodes in all the partial-wave functions of the $2P$ state, and the contributions of the wave functions before and after the nodes cancel each other, resulting in a very small branching ratio. In addition, the mass of $\bar{D}_2^{\star 0}(2P)$ is heavier than that of

TABLE V. Contributions of partial waves to the branching ratio of $B^+ \to \bar{D}_2^{\star 0}(1P)\ell^+\nu_\ell$ (in 10^{-4}).

	2^+			
0^-	Whole	P'-wave	D'-wave (B_1, B_2, B_7, B_8)	F'-wave
Whole	29.9	15.1	3.06	0.063
S-wave (A_1, A_2)	18.9	35.6	3.91	0.0026
P-wave (A_3, A_4)	1.48	4.45	10.1	0.048

TABLE VI. Contributions of partial waves to the branching ratio of $B^+ \to \bar{D}_2^{\star 0}(2P)\ell^+\nu_\ell$ (in 10^{-4}).

	2^+			
0^-	Whole	P'-wave	D'-wave (B_1, B_2, B_7, B_8)	F'-wave
Whole	0.752	0.0087	0.573	0.0033
S-wave (A_1, A_2)	0.015	0.0357	0.006	0.0001
P-wave (A_3, A_4)	0.557	0.0106	0.691	0.0026

$\bar{D}_2^{\star 0}(1P)$, and the phase space of the decay $B^+ \to \bar{D}_2^{\star 0}(2P)\ell^+\nu_\ell$ is smaller than that of $B^+ \to \bar{D}_2^{\star 0}(1P)\ell^+\nu_\ell$.

It can be seen from Table VI that the largest contribution does not come from the nonrelativistic term $S \times P'$, nor from the relativistic corrections $S \times D'$ and $P \times P'$, but from the relativistic correction $P \times D'$. The results show that the node structure has a more severe inhibitory effect on $S \times P'$ than on $P \times D'$, leading to the latter providing the maximum contribution and a large relativistic effect in this process.

3. $B_s^0 \to D_{s2}^{\star -}(1P)\ell^+\nu_\ell$

Table VII shows that, similar to the process of $B^+ \to \bar{D}_2^{\star 0}(1P)\ell^+\nu_\ell$, the overlap of $S \times P'$ provides the dominant contribution to $B_s^0 \to D_{s2}^{\star -}(1P)\ell^+\nu_\ell$, which is mainly nonrelativistic. All other contributions are relativistic corrections, with $P \times D'$ being the largest, followed by $S \times D'$ and $P \times P'$, while the contribution of F'-waves can be safely ignored. In the nonrelativistic limit, the branching ratio of $S \times P'$ should be changed from 48.0×10^{-4} in Table VII to 48.4×10^{-4}, so the relativistic effect is

$$\frac{\mathcal{B}_{\text{non-rel}} - \mathcal{B}_{\text{rel}}}{\mathcal{B}_{\text{rel}}} = 28.8\%, \tag{43}$$

which is also not as large as we expected, but a little larger than those of $B^+ \to \bar{D}_2^{\star 0}(1P)$. However, we cannot simply conclude that the relativistic effect of the former is greater than that of the latter. When we look at the details of relativistic corrections, compared with the nonrelativistic contribution, the contributions of $P \times D'$, $S \times D'$, and $P \times P'$ in the process $B_s^0 \to D_{s2}^{\star -}(1P)\ell^+\nu_\ell$ are much smaller than those in $B^+ \to \bar{D}_2^{\star 0}(1P)\ell^+\nu_\ell$, respectively. However, when summing them up, the overall result of the latter is smaller, due to cancellation.

4. $B_s^0 \to D_{s2}^{\star -}(2P)\ell^+\nu_\ell$

Table VIII illustrates the scenario of $B_s^0 \to D_{s2}^{\star -}(2P)\ell^+\nu_\ell$, which bears resemblance to the case of $B^+ \to \bar{D}_2^{\text{star}0}(2P)\ell^+\nu_\ell$. Notably, significant relativistic effects are observed. The primary contributions to the branching ratio arise from relativistic corrections, particularly the $P \times D'$ term, rather than nonrelativistic contributions.

TABLE VII. Contributions of partial waves to the branching ratio of $B_s^0 \to D_{s2}^{\star -}(1P)\ell^+\nu_\ell$ (in 10^{-4}).

	2^+			
0^-	Whole	P'-wave	D'-wave (B_1, B_2, B_7, B_8)	F'-wave
Whole	37.6	29.7	1.23	0.0359
S-wave (A_1, A_2)	29.0	48.0	2.90	0.0168
P-wave (A_3, A_4)	0.620	2.29	4.80	0.0309

TABLE VIII. Contributions of partial waves to the branching ratio of $B_s^0 \to D_{s2}^{\star -}(2P)\ell^+\nu_\ell$ (in 10^{-4}).

	2^+			
0^-	Whole	P'-wave	D'-wave (B_1, B_2, B_7, B_8)	F'-wave
Whole	1.24	0.137	0.546	0.00411
S-wave (A_1, A_2)	0.154	0.327	0.0241	0.00105
P-wave (A_3, A_4)	0.528	0.0414	0.789	0.00545

5. $B_c^+ \to \chi_{c2}(1P)\ell^+\nu_\ell$

In contrast to the value 21.9×10^{-4} of $S \times P'$ shown in Table IX, in the nonrelativistic limit, the branching ratio for $S \times P'$ is 22.2×10^{-4}, so we obtain

$$\frac{\mathcal{B}_{\text{non-rel}} - \mathcal{B}_{\text{rel}}}{\mathcal{B}_{\text{rel}}} = 22.1\% \tag{44}$$

for $B_c^+ \to \chi_{c2}(1P)\ell^+\nu_\ell$. This value seems not much different from that of $B^+ \to \bar{D}_2^{\star 0}(1P)\ell^+\nu_\ell$ or $B_s^0 \to D_{s2}^{\star -}(1P)\ell^+\nu_\ell$. However, from Tables V, VII, and IX, we can see that, although the complete branching ratios and nonrelativistic results do not differ significantly, each relativistic correction in $B_c^+ \to \chi_{c2}(1P)\ell^+\nu_\ell$ is much smaller than that in $B^+ \to \bar{D}_2^{\star 0}(1P)\ell^+\nu_\ell$ or in $B_s^0 \to D_{s2}^{\star -}(1P)\ell^+\nu_\ell$, respectively. We also note that the largest relativistic correction comes from $S \times D'$, not $P \times D'$.

6. $B_c^+ \to \chi_{c2}(2P)\ell^+\nu_\ell$

From Table X, we can see that, unlike the cases of $B^+ \to \bar{D}_2^{\star 0}(2P)\ell^+\nu_\ell$ and $B_s^0 \to D_{s2}^{\star -}(2P)\ell^+\nu_\ell$, the nonrelativistic

TABLE IX. Contributions of partial waves to the branching ratio of $B_c^+ \to \chi_{c2}(1P)\ell^+\nu_\ell$ (in 10^{-4}).

	2^+			
0^-	Whole	P'-wave	D'-wave (B_1, B_2, B_7, B_8)	F'-wave
Whole	18.2	19.1	0.110	0.00246
S-wave (A_1, A_2)	18.3	21.9	0.255	0.00012
P-wave (A_3, A_4)	0.0211	0.108	0.0761	0.00181

TABLE X. Contributions of partial waves to the branching ratio of $B_c^+ \to \chi_{c2}(2P)\ell^+\nu_\ell$ (in 10^{-4}).

	2^+			
0^-	Whole	P'-wave	D'-wave (B_1, B_2, B_7, B_8)	F'-wave
Whole	1.87	1.50	0.0245	0.00101
S-wave (A_1, A_2)	1.54	1.79	0.0241	0.00002
P-wave (A_3, A_4)	0.0169	0.0126	0.0523	0.00085

$S \times P'$ in $B_c^+ \to \chi_{c2}(2P)\ell^+\nu_\ell$ still contributes the most, much larger than the relativistic corrections, indicating that the node structure has different effects on the processes $B_c^+ \to \chi_{c2}(2P)\ell^+\nu_\ell$ and $B^+ \to \bar{D}_2^{\star 0}(2P)\ell^+\nu_\ell$ (or $B_s^0 \to D_{s2}^{\star -}(2P)\ell^+\nu_\ell$).

VI. CONCLUSION

We present a semirelativistic study on the semileptonic decays of heavy pseudoscalars B^+, B^0, B_s^0, and B_c^+ to $1P$, $2P$, and $3P$ 2^+ tensors caused by the transition of $\bar{b} \to \bar{c}$ by using the instantaneous Bethe-Salpeter method. We obtain $\mathcal{B}(B^+ \to \bar{D}_2^{\star 0}(1P)\ell^+\nu_\ell) = 2.99 \times 10^{-3}$ and $\mathcal{B}(B^0 \to \bar{D}_2^{\star -}(1P)\ell^+\nu_\ell) = 2.77 \times 10^{-3}$, which are in good agreement with the experimental data. For the undetected channels, our results are $\mathcal{B}(B_s^0 \to D_{s2}^{\star -}(1P)\ell^+\nu_\ell) = 3.76 \times 10^{-3}$ and $\mathcal{B}(B_c^+ \to \chi_{c2}(1P)\ell^+\nu_\ell) = 1.82 \times 10^{-3}$. For the decays to the $2P$ and $3P$ states, all branching ratios are very small and cannot be detected in current experiments.

In this paper, we focus on studying the different partial waves in the Salpeter wave functions and their contributions in semileptonic decays.

(1) In the wave function for the 0^- states, B^+, B^0, B_s^0, or B_c^+, the S-wave is dominant and provides the nonrelativistic contribution; the P-wave is sizable and gives the relativistic correction. While for the 2^+ states, $\bar{D}_2^{\star 0}$, $D_2^{\star -}$, $D_{s2}^{\star -}$, or χ_{c2}, the P-wave is dominant, combined with sizable D-wave, and tiny F-wave, where P-wave from ζ_5 and ζ_6 terms gives the nonrelativistic contribution, others contribute to the relativistic corrections.

(2) We note that, considering only the wave functions, the relativistic corrections for B, B_s, $\bar{D}_2^\star$, and $D_{s2}^\star$ mesons are large, while the relativistic corrections for χ_{c2} and B_c are small. However, when calculating the transition process, the overlapping integration of wave functions plays a major role. Thus, we obtain similar relativistic effects, for example, 24.4% for $B^+ \to \bar{D}_2^{\star 0}(1P)\ell^+\nu_\ell$, 28.8% for $B_s^0 \to D_{s2}^{\star -}(1P)\ell^+\nu_\ell$ and 22.1% for $B_c^+ \to \chi_{c2}(1P)\ell^+\nu_\ell$.

(3) When we look at the details, there are significant differences. For example, in the transition of $B \to D_2^\star(1P)$, the individual contributions of relativistic partial waves are significant, while in the overall result, they are in a canceling relationship, resulting in a small overall relativistic effect. While in $B_c^+ \to \chi_{c2}(1P)$, the individual contributions of relativistic waves are small, directly leading to a small overall relativistic effect.

(4) When the process contains a radially excited state, the node structure in the wave function of the radially excited state plays an overwhelming role, resulting in a very small branching ratio.

ACKNOWLEDGMENTS

This work was supported in part by the National Natural Science Foundation of China (NSFC) under the Grants No. 12075073, No. 12375085, and No. 11865001, the Natural Science Foundation of Hebei province under the Grant No. A2021201009.

APPENDIX: SALPETER EQUATIONS

$$
\begin{aligned}
MF_1(q_\perp) = {}& (\omega_1+\omega_2)F_1(q_\perp) + \int \frac{d\vec{k}}{(2\pi)^3}\frac{1}{24\omega_1\omega_2}\Bigg\{4(V_S-V_V)(e_1m_2+e_2m_1)\Bigg[-(F_3(k_\perp)-F_4(k_\perp)) \\
& - \frac{m_1-m_2}{e_1+e_2}(F_1(k_\perp)+F_2(k_\perp)) - \left(\frac{e_1-e_2}{m_1+m_2}(F_1(k_\perp)-F_2(k_\perp)) + (F_3(k_\perp)+F_4(k_\perp))\right)\frac{\omega_1+\omega_2}{e_1+e_2}\Bigg]\frac{q_\perp^2\vec{k}\cdot\vec{q}}{k_\perp^4} \\
& - 9(V_S+V_V)\left[(F_1(k_\perp)+F_2(k_\perp))(q_\perp^2+m_1m_2-\omega_1\omega_2) + (F_1(k_\perp)-F_2(k_\perp))(\omega_1m_2-\omega_2m_1)\frac{e_1-e_2}{m_1+m_2}\right] \\
& \times \left(\frac{(\vec{k}\cdot\vec{q})^2}{k_\perp^4} - \frac{q_\perp^2}{3k_\perp^2}\right) + 3(V_S-V_V)(e_1m_2+e_2m_1)\Bigg[(F_1(k_\perp)+F_2(k_\perp))\frac{5m_1+m_2}{e_1+e_2} + 2(F_3(k_\perp)-F_4(k_\perp)) \\
& + \left(\frac{5e_1+e_2}{m_1+m_2}(F_1(k_\perp)-F_2(k_\perp)) + 2(F_3(k_\perp)+F_4(k_\perp))\right)\frac{\omega_1+\omega_2}{e_1+e_2}\Bigg]\left(\frac{(\vec{k}\cdot\vec{q})^3}{k_\perp^6} - \frac{q_\perp^2\vec{k}\cdot\vec{q}}{3k_\perp^4}\right)\Bigg\}; \qquad \text{(A1)}
\end{aligned}
$$

$$
\begin{aligned}
MF_2(q_\perp) = & -(\omega_1+\omega_2)F_2(q_\perp) - \int \frac{d\vec{k}}{(2\pi)^3}\frac{1}{24\omega_1\omega_2}\Big\{4(V_S-V_V)(e_1m_2+e_2m_1)\Big[-(F_3(k_\perp)-F_4(k_\perp)) \\
& -\frac{m_1-m_2}{e_1+e_2}(F_1(k_\perp)+F_2(k_\perp)) + \left(\frac{e_1-e_2}{m_1+m_2}(F_1(k_\perp)-F_2(k_\perp)+(F_3(k_\perp)+F_4(k_\perp)))\right)\frac{\omega_1+\omega_2}{e_1+e_2}\Big]\frac{q_\perp^2\vec{k}\cdot\vec{q}}{k_\perp^4} \\
& -9(V_S+V_V)\left[(F_1(k_\perp)+F_2(k_\perp))(q_\perp^2+m_1m_2-\omega_1\omega_2)-(F_1(k_\perp)-F_2(k_\perp))(\omega_1m_2-\omega_2m_1)\frac{e_1-e_2}{m_1+m_2}\right] \\
& \times\left(\frac{(\vec{k}\cdot\vec{q})^2}{k_\perp^4}-\frac{q_\perp^2}{3k_\perp^2}\right)+3(V_S-V_V)(e_1m_2+3e_2m_1)\Big[(F_1(k_\perp)+F_2(k_\perp))\frac{5m_1+m_2}{e_1+e_2}+2(F_3(k_\perp)-F_4(k_\perp)) \\
& -\left(\frac{5e_1+e_2}{m_1+m_2}(F_1(k_\perp)-F_2(k_\perp))+2(F_3(k_\perp)+F_4(k_\perp))\right)\frac{\omega_1+\omega_2}{e_1+e_2}\Big]\left(\frac{(\vec{k}\cdot\vec{q})^3}{k_\perp^6}-\frac{q_\perp^2\vec{k}\cdot\vec{q}}{3k_\perp^4}\right)\Big\}; \qquad \text{(A2)}
\end{aligned}
$$

$$
\begin{aligned}
MF_3(q_\perp) = & (\omega_1+\omega_2)F_3(q_\perp) + \int \frac{d\vec{k}}{(2\pi)^3}\frac{1}{24\omega_1\omega_2}\Big\{-10(V_S+V_V)\Big[\Big(\frac{m_1-m_2}{m_1+m_2}\frac{e_1-e_2}{e_1+e_2} \\
& \times(F_1(k_\perp)+F_2(k_\perp))+\frac{e_1-e_2}{m_1+m_2}(F_3(k_\perp)-F_4(k_\perp))\Big)(m_2\omega_1-m_1\omega_2) \\
& +\left(\frac{e_1-e_2}{m_1+m_2}(F_1(k_\perp)-F_2(k_\perp))+(F_3(k_\perp)+F_4(k_\perp))\right)(q_\perp^2+m_1m_2-\omega_1\omega_2)\Big]\frac{(\vec{k}\cdot\vec{q})^2}{k_\perp^4} \\
& -8(V_S-V_V)\frac{e_2m_1+e_1m_2}{(e_1+e_2)(m_1+m_2)}[m_2((e_1-e_2)(F_1(k_\perp)-F_2(k_\perp))+(m_1+m_2)(F_3(k_\perp)+F_4(k_\perp))) \\
& +\omega_2((m_1-m_2)(F_1(k_\perp)+F_2(k_\perp))+(e_1+e_2)(F_3(k_\perp)-F_4(k_\perp)))]\frac{q_\perp^2\vec{k}\cdot\vec{q}}{k_\perp^4} \\
& +10(V_S-V_V)(e_2m_1+e_1m_2)\Big[\frac{e_1-e_2}{e_1+e_2}(F_1(k_\perp)-F_2(k_\perp))+\frac{m_1+m_2}{e_1+e_2}(F_3(k_\perp)+F_4(k_\perp)) \\
& +\frac{\omega_1+\omega_2}{m_1+m_2}\left(\frac{m_1-m_2}{e_1+e_2}(F_1(k_\perp)+F_2(k_\perp))+(F_3(k_\perp)-F_4(k_\perp))\right)\Big]\frac{q_\perp^2\vec{k}\cdot\vec{q}}{k_\perp^4} \\
& -2(V_S-V_V)(e_2m_1+e_1m_2)\Big[\frac{5e_1+e_2}{e_1+e_2}(F_1(k_\perp)-F_2(k_\perp))+2\frac{m_1+m_2}{e_1+e_2}(F_3(k_\perp)+F_4(k_\perp)) \\
& +\frac{\omega_1+\omega_2}{m_1+m_2}\left(\frac{5m_1+m_2}{e_1+e_2}(F_1(k_\perp)+F_2(k_\perp))+2(F_3(k_\perp)-F_4(k_\perp))\right)\Big]\frac{q_\perp^2\vec{k}\cdot\vec{q}}{k_\perp^4} \\
& +3(V_S+V_V)\Big[(F_1(k_\perp)+F_2(k_\perp))(m_1\omega_2-m_2\omega_1)-\frac{e_1-e_2}{m_1+m_2}(F_1(k_\perp)-F_2(k_\perp)) \\
& \times(-q_\perp^2+m_1m_2-\omega_1\omega_2)\Big]\left(\frac{q_\perp^2}{k_\perp^2}-\frac{3(\vec{k}\cdot\vec{q})^2}{k_\perp^4}\right)+(V_S+V_V)\frac{1}{m_1+m_2}\Big[\frac{e_1-e_2}{e_1+e_2}((m_1-m_2) \\
& \times(F_1(k_\perp)+F_2(k_\perp))+(e_1+e_2)(F_3(k_\perp)-F_4(k_\perp)))(m_2\omega_1-m_1\omega_2)+((e_1-e_2) \\
& \times(F_1(k_\perp)-F_2(k_\perp))+(m_1+m_2)(F_3(k_\perp)+F_4(k_\perp)))(q_\perp^2+m_1m_2-\omega_1\omega_2)\Big] \\
& \times\left(\frac{3q_\perp^2}{k_\perp^2}+\frac{(\vec{k}\cdot\vec{q})^2}{k_\perp^4}\right)+2(V_S-V_V)\frac{e_2m_1+e_1m_2}{(e_1+e_2)(m_1+m_2)}[m_2((5e_1+e_2)(F_1(k_\perp)-F_2(k_\perp)) \\
& +2(m_1+m_2)(F_3(k_\perp)+F_4(k_\perp)))+\omega_2((5m_1+m_2)(F_1(k_\perp)+F_2(k_\perp)) \\
& +2(e_1+e_2)(F_3(k_\perp)-F_4(k_\perp)))]\left(\frac{3(\vec{k}\cdot\vec{q})^3}{k_\perp^6}-\frac{q_\perp^2\vec{k}\cdot\vec{q}}{k_\perp^4}\right)\Big\}; \qquad \text{(A3)}
\end{aligned}
$$

$$
\begin{aligned}
MF_4(q_\perp) = &-(\omega_1+\omega_2)F_4(q_\perp) - \int \frac{d\vec{k}}{(2\pi)^3}\frac{1}{24\omega_1\omega_2}\Big\{-10(V_S+V_V)\Big[\Big(-\frac{m_1-m_2}{m_1+m_2}\frac{(e_1-e_2)}{(e_1+e_2)} \\
&\times(F_1(k_\perp)+F_2(k_\perp)) + \frac{e_1-e_2}{m_1+m_2}(F_3(k_\perp)-F_4(k_\perp))\Big)(m_2\omega_1-m_1\omega_2) \\
&+\Big(\frac{e_1-e_2}{m_1+m_2}(F_1(k_\perp)-F_2(k_\perp)) + (F_3(k_\perp)+F_4(k_\perp))\Big)(q_\perp^2+m_1m_2-\omega_1\omega_2)\Big]\frac{(\vec{k}\cdot\vec{q})^2}{k_\perp^4} \\
&-8(V_S-V_V)\frac{(e_2m_1+e_1m_2)}{(e_1+e_2)(m_1+m_2)}[m_2((e_1-e_2)(F_1(k_\perp)-F_2(k_\perp))+(m_1+m_2)(F_3(k_\perp)+F_4(k_\perp))) \\
&-\omega_2((m_1-m_2)(F_1(k_\perp)+F_2(k_\perp))+(e_1+e_2)(F_3(k_\perp)-F_4(k_\perp)))]\frac{q_\perp^2\vec{k}\cdot\vec{q}}{k_\perp^4} \\
&+10(V_S-V_V)(e_2m_1+e_1m_2)\Big[\frac{e_1-e_2}{e_1+e_2}(F_1(k_\perp)-F_2(k_\perp)) + \frac{m_1+m_2}{e_1+e_2}(F_3(k_\perp)+F_4(k_\perp)) \\
&-\frac{\omega_1+\omega_2}{m_1+m_2}\Big(\frac{m_1-m_2}{e_1+e_2}(F_1(k_\perp)+F_2(k_\perp)) + (F_3(k_\perp)-F_4(k_\perp))\Big)\Big]\frac{q_\perp^2\vec{k}\cdot\vec{q}}{k_\perp^4} \\
&-2(V_S-V_V)(e_2m_1+e_1m_2)\Big[\frac{5e_1+e_2}{e_1+e_2}(F_1(k_\perp)-F_2(k_\perp)) + 2\frac{m_1+m_2}{e_1+e_2}(F_3(k_\perp)+F_4(k_\perp)) \\
&-\frac{\omega_1+\omega_2}{m_1+m_2}\Big(\frac{5m_1+m_2}{e_1+e_2}(F_1(k_\perp)+F_2(k_\perp)) + 2(F_3(k_\perp)-F_4(k_\perp))\Big)\Big]\frac{q_\perp^2\vec{k}\cdot\vec{q}}{k_\perp^4} \\
&+3(V_S+V_V)\Big[-(F_1(k_\perp)+F_2(k_\perp))(m_1\omega_2-m_2\omega_1) - \frac{e_1-e_2}{m_1+m_2}(F_1(k_\perp)-F_2(k_\perp)) \\
&\times(-q_\perp^2+m_1m_2-\omega_1\omega_2)\Big]\Big(\frac{q_\perp^2}{k_\perp^2}-\frac{3(\vec{k}\cdot\vec{q})^2}{k_\perp^4}\Big) + (V_S+V_V)\frac{1}{m_1+m_2}\Big[-\frac{e_1-e_2}{e_1+e_2}((m_1-m_2) \\
&\times(F_1(k_\perp)+F_2(k_\perp)) + (e_1+e_2)(F_3(k_\perp)-F_4(k_\perp)))(m_2\omega_1-m_1\omega_2) + ((e_1-e_2) \\
&\times(F_1(k_\perp)-F_2(k_\perp)) + (m_1+m_2)(F_3(k_\perp)+F_4(k_\perp)))(q_\perp^2+m_1m_2-\omega_1\omega_2)\Big] \\
&\times\Big(\frac{3q_\perp^2}{k_\perp^2}+\frac{(\vec{k}\cdot\vec{q})^2}{k_\perp^4}\Big) + 2(V_S-V_V)\frac{e_2m_1+e_1m_2}{(e_1+e_2)(m_1+m_2)}[m_2((5e_1+e_2)(F_1(k_\perp)-F_2(k_\perp)) \\
&+2(m_1+m_2)(F_3(k_\perp)+F_4(k_\perp))) - \omega_2((5m_1+m_2)(F_1(k_\perp)+F_2(k_\perp)) \\
&+2(e_1+e_2)(F_3(k_\perp)-F_4(k_\perp)))]\Big(\frac{3(\vec{k}\cdot\vec{q})^3}{k_\perp^6}-\frac{q_\perp^2\vec{k}\cdot\vec{q}}{k_\perp^4}\Big)\Big\}. \qquad \text{(A4)}
\end{aligned}
$$

Here, $e_i = \sqrt{m_i^2+k_T^2}$, $V_S = V_S(\vec{q}-\vec{k})$ and $V_V = V_V(\vec{q}-\vec{k})$. When solving the Salpeter equations (A1)–(A4), since the radial wave function $\zeta_i(\vec{q}^2)$ or $F_i(\vec{q}^2)$ decreases with the increase of $|\vec{q}|$ (see Fig. 3 for example), we truncate the relative momentum $|\vec{q}|$ (and $|\vec{k}|$) to a certain maximum value $|\vec{q}|_{\max}$ ($|\vec{k}|_{\max} = |\vec{q}|_{\max}$), and discretize this momentum into n parts (n is a large number). Thus, the four coupled eigenvalue equations were transformed into a $4n\times4n$ matrix formula, and then the numerical solutions were implemented.

[1] W. Wang, Y.-L. Shen, C.-D. Lv, M. A. Paracha, and C. Wang, Phys. Rev. D **79**, 054012 (2009).
[2] R.-H. Li, C.-D. Lv, and H. Zou, Phys. Rev. D **78**, 014018 (2008).
[3] X.-W. Kang, T. Luo, Y. Zhang, L.-Y. Dai, and C. Wang, Eur. Phys. J. C **78**, 909 (2018).
[4] J. Dingfelder and T. Mannel, Rev. Mod. Phys. **88**, 035008 (2016).
[5] T. M. Aliev, K. Azizi, and A. Ozpineci, Eur. Phys. J. C **51**, 593 (2007).
[6] B. Aubert *et al.* (*BABAR* Collaboration), Phys. Rev. Lett. **101**, 261802 (2008).
[7] R. Van Tonder *et al.* (Belle Collaboration), Phys. Rev. D **104**, 112011 (2021).
[8] J. P. Lees *et al.* (*BABAR* Collaboration), Phys. Rev. D **85**, 011101 (2012).
[9] V. M. Abazov *et al.* (D0 Collaboration), Phys. Rev. Lett. **102**, 051801 (2009).
[10] R. Aaij *et al.* (LHCb Collaboration), J. High Energy Phys. 07 (2020) 123.
[11] R. Aaij *et al.* (LHCb Collaboration), J. High Energy Phys. 01 (2022) 065.
[12] F. Abudinén *et al.* (Belle-II Collaboration), Phys. Rev. D **107**, 072002 (2023).
[13] D. Bigi, P. Gambino, and S. Schacht, J. High Energy Phys. 11 (2017) 061.
[14] B. Aubert *et al.* (*BABAR* Collaboration), Phys. Rev. Lett. **87**, 091801 (2001).
[15] K. Abe *et al.* (Belle Collaboration), Phys. Rev. Lett. **87**, 091802 (2001).
[16] S. Fajfer, J. F. Kamenik, and I. Nisandzic, Phys. Rev. D **85**, 094025 (2012).
[17] Z.-R. Huang, Y. Li, C.-D. Lv, M. A. Paracha, and C. Wang, Phys. Rev. D **98**, 095018 (2018).
[18] D. Scora and N. Isgur, Phys. Rev. D **52**, 2783 (1995).
[19] V. Morenas, A. Le Yaouanc, L. Oliver, O. Pene, and J. C. Raynal, Phys. Rev. D **56**, 5668 (1997).
[20] P. Colangelo, F. De Fazio, and N. Paver, Phys. Rev. D **58**, 116005 (1998).
[21] I. I. Bigi, B. Blossier, A. Le Yaouanc, L. Oliver, O. Pene, J. C. Raynal, A. Oyanguren, and P. Roudeau, Eur. Phys. J. C **52**, 975 (2007).
[22] G.-L. Wang, Q. Li, T. Wang, T.-F. Feng, X.-G. Wu, and C.-H. Chang, Eur. Phys. J. C **82**, 1027 (2022).
[23] G.-L. Wang, T.-F. Feng, and X.-G. Wu, Phys. Rev. D **101**, 116011 (2020).
[24] E. E. Salpeter and H. A. Bethe, Phys. Rev. **84**, 1232 (1951).
[25] E. E. Salpeter, Phys. Rev. **87**, 328 (1952).
[26] C. S. Kim and G.-L. Wang, Phys. Lett. B **584**, 285 (2004).
[27] G.-L. Wang, Phys. Lett. B **674**, 172 (2009).
[28] C.-H. Chang and G.-L. Wang, Sci. China Phys. Mech. Astron. **53**, 2005 (2010).
[29] E. Eichten, K. Gottfried, T. Kinoshita, K. D. Lane, and T. M. Yan, Phys. Rev. D **17**, 3090 (1978); **21**, 313(E) (1980).
[30] G.-L. Wang, T. Wang, Q. Li, and C.-H. Chang, J. High Energy Phys. 05 (2022) 006.
[31] T.-T. Liu, S.-Y. Pei, W. Li, M. Han, and G.-L. Wang, Eur. Phys. J. C **82**, 737 (2022).
[32] W. Li, S.-Y. Pei, T. Wang, Y.-L. Wang, T.-F. Feng, and G.-L. Wang, Phys. Rev. D **107**, 113002 (2023).
[33] S.-Y. Pei, W. Li, T.-T. Liu, M. Han, G.-L. Wang, and T.-H. Wang, Phys. Rev. D **108**, 033003 (2023).
[34] R. L. Workman *et al.* (Particle Data Group), Prog. Theor. Exp. Phys. **2022**, 083C01 (2022).
[35] C.-H. Chang, J.-K. Chen, and G.-L. Wang, Commun. Theor. Phys. **46**, 467 (2006).
[36] V. Morenas, A. Le Yaouanc, L. Oliver, O. Pene, and J.-C. Raynal, Phys. Rev. D **56**, 5668 (1997).
[37] T. M. Aliev, H. Dag, A. Kokulu, and A. Ozpineci, Phys. Rev. D **100**, 094005 (2019).
[38] K. Azizi, H. Sundu, and S. Sahin, Phys. Rev. D **88**, 036004 (2013).
[39] L.-L. Chen, Y.-W. Ren, L.-T. Wang, and Q. Chang, Eur. Phys. J. C **82**, 451 (2022).
[40] M. Oda, K. Nishimura, M. Ishida, and S. Ishida, Prog. Theor. Phys. **103**, 1213 (2000).
[41] D. Scora and N. Isgur, Phys. Rev. D **52**, 2783 (1995).
[42] D. Ebert, R. N. Faustov, and V. O. Galkin, Phys. Rev. D **61**, 014016 (2000).
[43] H.-R. Dong, A. Le Yaouanc, L. Oliver, and J.-C. Raynal, Phys. Rev. D **90**, 114014 (2014).
[44] T. Barakat, Nucl. Phys. **B983**, 115915 (2022).
[45] K. Azizi, H. Sundu, and S. Sahin, Eur. Phys. J. C **75**, 197 (2015).
[46] R. N. Faustov and V. O. Galkin, Phys. Rev. D **87**, 034033 (2013).
[47] J. Segovia, C. Albertus, D. R. Entem, F. Fernandez, E. Hernandez, and M. A. Perez-Garcia, Phys. Rev. D **84**, 094029 (2011).
[48] D. Ebert, R. N. Faustov, and V. O. Galkin, Phys. Rev. D **82**, 034019 (2010).
[49] M. A. Ivanov, J. G. Korner, and P. Santorelli, Phys. Rev. D **73**, 054024 (2006).
[50] E. Hernandez, J. Nieves, and J. M. Verde-Velasco, Phys. Rev. D **74**, 074008 (2006).
[51] C.-H. Chang, Y.-Q. Chen, G.-L. Wang, and H.-S. Zong, Phys. Rev. D **65**, 014017 (2002).
[52] S.-C. Zhang, T. Wang, Y. Jiang, Q. Li, and G.-L. Wang, Int. J. Mod. Phys. A **32**, 1750022 (2017).